Mechanistic investigations of matrix metalloproteinase-8 inhibition by metal abstraction peptide

Jenifer K. Tucker
Bioengineering Research Center, University of Kansas, Lawrence, Kansas 66045 and Department of Chemistry, University of Kansas, Lawrence, Kansas 66045

Michaela L. McNiff
Department of Pharmaceutical Chemistry, University of Kansas, Lawrence, Kansas 66047

Sasanka B. Ulapane
Bioengineering Research Center, University of Kansas, Lawrence, Kansas 66045 and Department of Chemistry, University of Kansas, Lawrence, Kansas 66045

Paulette Spencer
Bioengineering Research Center, University of Kansas, Lawrence, Kansas 66045 and Department of Mechanical Engineering, University of Kansas, Lawrence, Kansas 66045

Jennifer S. Laurence[a)]
Bioengineering Research Center, University of Kansas, Lawrence, Kansas 66045 and Department of Pharmaceutical Chemistry, University of Kansas, Lawrence, Kansas 66047

Cindy L. Berrie[a)]
Bioengineering Research Center, University of Kansas, Lawrence, Kansas 66045 and Department of Chemistry, University of Kansas, Lawrence, Kansas 66045

(Received 3 February 2016; accepted 18 April 2016; published 29 April 2016)

The mechanism of matrix metalloproteinase-8 (MMP-8) inhibition was investigated using ellipsometric measurements of the interaction of MMP-8 with a surface bound peptide inhibitor, tether-metal abstraction peptide (MAP), bound to self-assembled monolayer films. MMP-8 is a collagenase whose activity and dysregulation have been implicated in a number of disease states, including cancer metastasis, diabetic neuropathy, and degradation of biomedical reconstructions, including dental restorations. Regulation of activity of MMP-8 and other matrix metalloproteinases is thus a significant, but challenging, therapeutic target. Strong inhibition of MMP-8 activity has recently been achieved via the small metal binding peptide tether-MAP. Here, the authors elucidate the mechanism of this inhibition and demonstrate that it occurs through the direct interaction of the MAP Tag and the Zn^{2+} binding site in the MMP-8 active site. This enhanced understanding of the mechanism of inhibition will allow the design of more potent inhibitors as well as assays important for monitoring critical MMP levels in disease states. © *2016 American Vacuum Society*. [http://dx.doi.org/10.1116/1.4948340]

I. INTRODUCTION

Matrix metalloproteinases (MMPs), including MMP-8, are proteinases that degrade extracellular matrix (ECM) proteins as well as other non-ECM proteins.[1] They are crucial for normal biological function, but changes in the levels and activity of MMPs have been associated with a variety of disease states, including cancer metastasis, atherosclerosis, diabetes, periodontal inflammation, pulmonary fibrosis, and tuberculosis.[2–8] In addition, MMPs have been implicated in the degradation of biomedical implants including dental restorations.[3,4,8–10] MMP-8 degrades collagen and has been shown to be activated and to degrade the tooth structure around dental restorations (specifically the type I collagen in dentin).[8] Regulation of MMP-8 and other matrix metalloproteinases is therefore a significant therapeutic target.[4–7]

Although the activity of MMP-8 is naturally regulated by inhibitory proteins, dysregulation of MMP-8 has been found in a variety of disease states, and thus, development of specific small molecule and peptide-based inhibitors for these MMPs has been an active area of research.[11–15] MMP-8 contains a large binding pocket with a flexible loop which has hindered the development of very tight binding inhibitors.[15] It has recently been demonstrated that a small peptide containing a metal binding sequence, tether-metal abstraction peptide (MAP), grafted to dental adhesive polymer formulations, is a potent, effective inhibitor of MMP-8 activity, but the mechanism of inhibition is not known.[16] Several possibilities exist for the mechanism of action of this peptide-based inhibitor including direct binding of the metal binding MAP Tag within the Zn^{2+} binding pocket of MMP-8 [Fig. 1(a)] or abstraction of the zinc ion from MMP-8, resulting in inactivation of the enzyme [Fig. 1(b)].

Understanding the mechanism of action is critical for future developments of inhibitors and their implementation in biomedical reconstructions, devices, and therapies. In this work, we demonstrate using ellipsometric studies at model self-assembled monolayer (SAM) surfaces (Fig. 2) that there is a direct interaction between the tether-MAP peptide and MMP-8, which results in MMP-8 binding to the peptide-coated

[a)]Authors to whom correspondence should be addressed; electronic addresses: cberrie@ku.edu; laurencj@ku.edu

surface. Specifically, we have coupled the tether-MAP peptide to amine-terminated SAM films via linking of the peptide with the amine group on the surface through a disuccinimidyl suberate (DSS) crosslinker [Fig. 2(a)]. Additionally, we utilized control hydroxyl-terminated SAM surfaces, which do not bind peptide, [Fig. 2(b)] for investigation of nonspecific interactions of MMP-8 with the surface. The thickness of the films is monitored at each step using ellipsometry. An increase in thickness is observed when MMP-8 is deposited on the peptide coated amine-terminated SAM but not on the control surfaces. Furthermore, this interaction can be prevented by blocking the metal binding site of the peptide with Ni^{2+}, which suggests that the interaction specifically occurs through the metal binding MAP Tag at the Zn^{2+} binding pocket of the enzyme.

II. EXPERIMENT

A. Materials

Gold substrates (4 in. diameter 525 μm thick silicon wafers with 100 nm of gold deposited with titanium adhesion layer) were obtained from Platypus Technologies (Au.1000.SL1). Thiols including 11-amino-1-undecanethiol, hydrochloride ($R\text{-}NH_2$) and 11-mercapto-1-undecanol (R-OH) were obtained from Sigma-Aldrich. Dimethyl sulfoxide (DMSO), triethylamine, sodium phosphate dibasic, sodium hydroxide (NaOH), sodium dodecyl sulfate (SDS), Triton X-100 (Triton), and ethylenediaminetetraacetic acid (EDTA) were obtained from Sigma-Aldrich. Two-hundred proof ethanol was obtained from Decon laboratories. (4-(2-hydroxyethyl)-1-piperazineethane sulfonic acid) (HEPES), sodium chloride, potassium chloride, potassium phosphate monobasic, Tris base, hydrochloric acid (HCl), chloroform, acetone, acetic acid, nickel sulfate hexahydrate, and zinc sulfate were obtained from Fisher Scientific. DSS, a homobifunctional crosslinker, was obtained from ProteoChem. Milli-Q water (resistivity >17 M$\Omega \cdot$ cm) was used throughout.

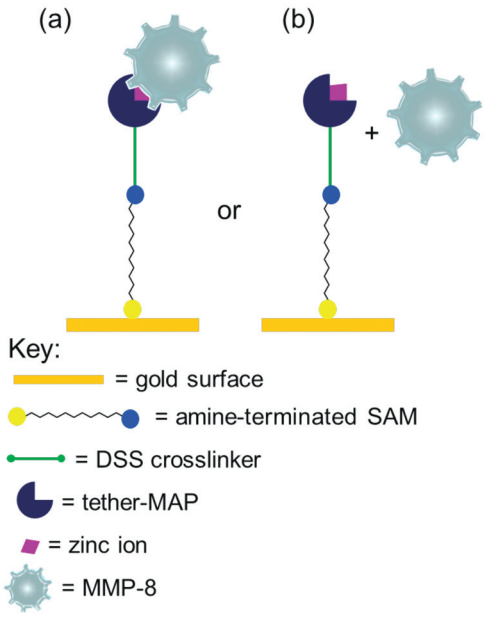

FIG. 1. Potential mechanisms of MMP-8 inhibition by tether-MAP peptide. (a) Shared Zn^{2+} binding between MMP-8 and tether-MAP, or (b) Abstraction of Zn^{2+} from MMP-8 by tether-MAP.

Peptide SWLAYPGAVSYRG*NCC* (tether-MAP) was custom synthesized by GenScript (>95% purity), provided in small aliquots and stored at −20 °C to reduce freeze/thaw cycles of the peptide. Peptide was allowed to equilibrate to room temperature prior to hydration and use.

1. MMP-8 protein production

The catalytic domain of MMP-8 was engineered into a fusion construct and the protein expressed in *Escherichia coli* as previously described.[17] In the present study, two variants of MMP-8 were used. Both contain an *N*-terminal thioredoxin-S Tag fusion partner and a polyhistidine tag for purification (MMP-8 fusion), and in addition, one contained the metal-binding *cla*MP Tag and a spacer sequence inserted between the fusion partner and MMP-8 (*cla*MP-link-MMP-8 fusion). Immobilized metal affinity chromatography was used to purify the fusion protein from the soluble fraction of the cell lysate. The thioredoxin and S Tag were cleaved by thrombin and Factor Xa to release MMP-8 (which also removed the polyhistidine purification tag). Catalytic activity was determined using MMP-8 Fluorescent Drug Discovery Kit, RED (Enzo Life Sciences) according to the manufacturer's instructions. Complete inhibition of the fusion enzyme was accomplished using *N*-Isobutyl-*N*-(4-methoxyphenylsulfonyl)glycyl hydroxamic acid (NNGH).

2. Buffers

HEPES buffer *p*H 7.4 (20 mM HEPES, 200 mM potassium chloride, *p*H adjusted to 7.4 with 1 M NaOH), potassium phosphate buffer *p*H 7.4 (137 mM NaCl, 2.7 mM KCl, 10 mM Na_2HPO_4, and 1.8 mM KH_2PO_4, *p*H adjusted to 7.4 with 1 M NaOH), Tris buffer (20–200 mM Tris base, *p*H adjusted to 7.4 with 1 M HCl), protein buffer (50 mM Tris-Cl, 60 mM NaCl buffer, *p*H 7.9), Enzo Life Sciences MMP-8 Fluorometric Drug Discovery Kit, RED assay buffer (50 mM HEPES, 10 mM $CaCl_2$, 0.05% Brij-35, *p*H 7.5), and acetate buffers (50 mM acetate buffer *p*H 3.5, 50 mM acetate buffer *p*H 3.5 with 10 mM EDTA, 50 mM acetate buffer *p*H 4.5 with 10 mM EDTA) were all utilized.

B. Methods

1. Ellipsometry

Film thicknesses were determined under ambient conditions using a single wavelength Rudolf Auto EL III ellipsometer at a wavelength of 632.8 nm with an incident angle of 70°. For each sample, averaged optical constants determined from measurements at 5–7 different spots for each gold piece were determined on each freshly cleaned gold sample. The optical constants showed some variability among different gold samples but typical values were $n = 1.5$ and $k = 3.5$. A refractive index of $n = 1.465$ was assumed for the organic, peptide, and protein layers for all

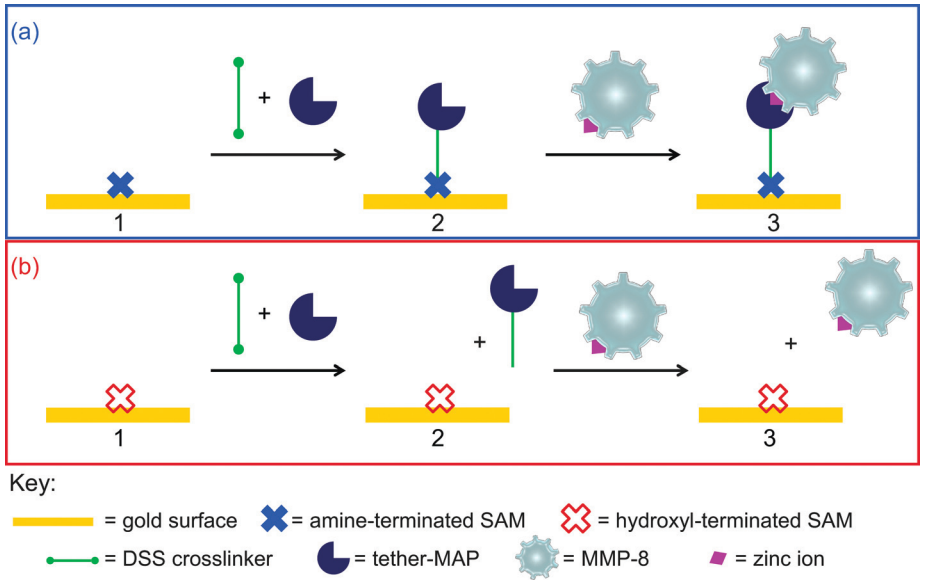

FIG. 2. Schematic of binding studies on (a) amine-terminated SAM and (b) hydroxyl-terminated (control) SAM films. For each scheme: Step (1) initial SAM film, (2) after tether-MAP coupling, and (3) after MMP-8 incubation.

samples.[18–20] Additionally, a negligible absorptivity of the films ($k = 0$) at the wavelength of the measurement (632.8 nm) was assumed. This has been verified with UV-Vis measurements of the peptide and protein (unpublished data). Approximately five to seven measurements at different spots on the surface were obtained for each sample with a minimum of three different samples for each surface termination (amine and hydroxyl).

2. Contact angle goniometry

Static water contact angles were determined via goniometry using a Ramé Hart goniometer by adding deionized water to the surface to form a drop and measuring the contact angle between the surface and water from both sides of this water droplet. This was performed in triplicate with water droplets randomly distributed on each surface.

3. SAM film formation

Gold substrate samples of approximately 1–3 cm^2 were cut from gold wafers using a diamond-tipped scribe. These samples were rinsed with deionized water and dried with nitrogen gas. Gold substrates were rinsed with chloroform, acetone, and ethanol and then dried with nitrogen gas. Optical constants for each gold substrate were obtained via ellipsometry. Gold substrates were then rinsed with solvents again. SAMs were prepared by immersing these cleaned gold substrates into respective thiol solutions for a minimum of 24 h. At least three replicate samples were prepared for each experiment. Hydroxyl-terminated thiol (11-mercapto-1-undecanol, HS-$(CH_2)_{11}$-OH or R-OH) solutions (2 mM) with ethanol as the solvent were prepared as control samples. Amine-terminated thiol (11-amino-1-undecanethiol, hydrochloride, HS-$(CH_2)_{11}$-NH_2·HCl or R-NH_2) solutions of 0.5 mM in ethanol spiked with 3% triethylamine were prepared (conditions to minimize bilayer formation).[21] After incubation, R-OH samples were removed from solution, rinsed with ethanol and water, and dried with nitrogen gas. Samples incubated in R-NH_2 thiol were removed from solution, rinsed with ethanol, acetic acid (to disrupt any potential bilayer formation), and ethanol again, and dried with nitrogen gas. Thicknesses of monolayer samples were measured via ellipsometry and contact angles were measured via goniometry to verify functionalization of the gold surfaces.[21–27] See Table I for values of typical initial thicknesses and contact angles for each type of monolayer sample. The slightly larger thickness of the R-NH_2 sample relative to the R-OH samples is likely the result of either partial bilayer formation on the amine sample or differences in packing between the two samples. This difference is reproducibly observed from sample to sample and consistent with previous literature. In addition, AFM measurements on similar samples indicate RMS roughness values comparable to the bare gold substrates used (~1 nm) on both types of samples.

4. Mixed SAMs formation

Mixed SAMs were prepared in mixtures of 10:90 (0.2:2 mM), 25:75 (0.5:2 mM), and 50:50 (0.5:0.5 mM) of R-NH_2:R-OH to make SAMs approximately 10%, 25%, and 50% amine-terminated, respectively. All mixed thiol solutions contained the 3% triethylamine spike. Gold surfaces and SAMs were prepared and characterized as above for the 100% SAMs (Table I).

5. Coupling of peptide to surfaces

DSS was used to covalently couple the N-terminal amine of the peptide (tether-MAP) to the amine-terminated surface groups. To perform this step, directions from ProteoChem's Product Information Sheet and General Protocol were followed with slight modifications. A stock solution of 1–2 mg/

TABLE I. Typical thicknesses and contact angles for SAM films.

SAM (R-NH_2:R-OH)	Thickness (Å)	Contact angle (deg)
R-OH	11.9 ± 0.8	21 ± 1
10:90	12.9 ± 0.6	22 ± 4
25:75	13.8 ± 0.8	23 ± 2
50:50	17.4 ± 0.7	32 ± 1
R-NH_2	18.8 ± 1.1	45 ± 3[a]

[a]Contact angles as low as 25° have been observed on some samples.

ml (or 0.57–1.1 mM) tether-MAP was prepared in potassium phosphate buffer *p*H 7.4. Ninety-four microliters of 20 mM HEPES buffer *p*H 7.4 was added to each sample surface. This was followed by sequential addition and mixing of 4 μl of 0.57–1.1 mM tether-MAP in buffer and typically 2 μl 50–75 mM DSS in DMSO. Samples were incubated in a covered container protected from light for approximately 60–75 min (increased from manufacturer's recommendation to allow time for diffusion and reaction at the surface). Variability in the DSS activity was observed from lot to lot, and thus, optimization of the DSS concentration for each batch was required.

The reaction was quenched with 50–100 μl of 20–200 mM Tris buffer (for approximately 15 min). Samples were then rinsed with HEPES buffer and water and dried with nitrogen gas. To remove nonspecifically bound peptide and/or cross-linker, samples were incubated in a mixture of 0.5% SDS with 0.5% Triton for approximately 20–60 min. Samples were rinsed three times with 0.5% SDS and then with buffer and deionized water before being dried with nitrogen gas and characterized using ellipsometry.

6. MMP-8 and tether-MAP interaction

To observe potential interaction of MMP-8 with the tether-MAP, MMP-8 was diluted in protein buffer to make secondary stock solutions and then further diluted five-fold to a range of concentrations between 0.01 and 10 μM in Enzo kit assay buffer. This diluted protein of 50–100 μl was placed on each sample surface for 100–110 min. After incubation, samples were rinsed with HEPES buffer and water and dried with nitrogen gas. Ellipsometry was utilized to characterize the samples.

7. Removal of surface bound MMP-8

Attempts were made to remove MMP-8 bound to the surface by soaking samples in denaturing solution (either 0.5% SDS or 0.5% SDS/0.5% Triton) for 30–60 min. Metal binding to MAP requires neutral to basic *p*H.[28] Therefore, samples were subsequently rinsed with acetate buffers *p*H 3.5, *p*H 3.5 with EDTA, and *p*H 4.5 with EDTA, and then incubated in acetate buffer *p*H 4.5 with EDTA for several hours to disrupt MAP binding to Zn^{2+}.

III. RESULTS AND DISCUSSION

Inhibition of MMP-8 by the tether-MAP peptide has been demonstrated previously, but the mechanism for this inhibition had not yet been investigated. Based on knowledge of the MAP chemistry, two likely possibilities exist for the mechanism of MMP-8 inhibition including: (1) shared binding of the zinc ion in MMP-8's active site by the MAP sequence or (2) removal by abstraction of the zinc ion from the catalytic portion of the MMP-8 by the MAP Tag (Fig. 1). This ellipsometric study was designed to test the mechanism for MMP-8 inhibition by tether-MAP. Should the substantially larger 18-kDa MMP-8 protein bind to the peptide on the tether-MAP-modified SAM surface, a significant increase in height would be expected after the protein incubation step. If the peptide abstracts zinc ions from the MMP-8, a very minimal change in height would be expected because the protein would diffuse away from the surface rather than remain bound and the small size zinc ion remaining would not result in a measurable thickness change (Fig. 6). We used model SAM surfaces and ellipsometry to investigate this inhibition mechanism by determining the thickness of the surface bound film at each stage in the experiment.

A. Protein preparation

Sufficient quantities of active, pure MMP-8 are not available commercially at an affordable price for such mechanistic investigations. Our group has recently developed methods of preparing a relatively stable, active, inhibitable MMP-8 fusion construct.[17] Two different protein variants were used in the investigations described here: *cla*MP-link-MMP-8 fusion and MMP-8 fusion.[17] Each of these proteins has been characterized extensively and shown to be catalytically active and inhibited by the standard inhibitor NNGH, both in the fusion construct and following cleavage to release the tags. Once the fusion partner in each of these constructs is cleaved to release the MMP-8 domain, significant fragmentation of the enzyme is observed over time along with a decrease in activity. While the cleaved MMP-8 constructs degrade with time, they retain catalytic activity for time periods long enough for experiments such as those described here. Separation of residual intact fusion protein is easily achieved, but in the cleaved samples used in these studies, a mixture of MMP-8 cleavage fragments remains. For these reasons, two different catalytically active protein variants with different cleavage fragments were used to verify that the results obtained in this study are not due to the fusion partner or residual contamination with other fragments. Because of the significant degradation products and cleavage fragments, the protein concentrations reported here reflect total protein content in the sample, not the concentration of intact MMP-8, which may vary from batch to batch. Stability analysis confirms that the activity is retained with cold storage for several days. Experiments were run within 4 days after cleavage, and protein was typically stored refrigerated until samples were used to minimize the amount of degradation. Based on the characterization of activity and stability presented in McNiff *et al.*,[17] sufficient quantities of active MMP-8 are present in these samples to investigate the mechanism of interaction between MMP-8 and tether-MAP.

B. Surface coupling of peptide inhibitor

Experiments were carried out in parallel on hydroxyl- and amine-terminated SAMs (or mixtures thereof), as shown in Fig. 2. Briefly, SAMs were characterized, exposed to the crosslinking solution for tether-MAP attachment, rinsed, dried, and characterized. Additionally, mixed SAMs were used to determine if packing density might impact the peptide–protein interaction.

SAMs were initially characterized via ellipsometry and goniometry to confirm the formation of the monolayers and determine the packing adequacy as well as wettability. Initial values (Table I) were similar to literature values.[21–27] Next, peptide was grafted to the surface of the SAM using a homobifunctional crosslinker, DSS, which consists of a linker with an amine-reactive *N*-hydroxysuccinimide ester group at each end. These esters will form amide bonds with primary amine groups, releasing the *N*-hydroxysuccinimide groups in the process. The N-terminal amine of the tether-MAP peptide was grafted to the amine-terminal group on the amine containing surfaces via this crosslinker (while no reaction was expected on the hydroxyl-terminated surfaces). Figure 3 shows that when the tether-MAP peptide is coupled to the amine-terminated SAM film, a large increase in thickness is observed, but no increase is observed in the case of the hydroxyl-terminated films. On the amine-terminated SAM, this orients the peptide such that the MAP Tag is exposed at the surface and available for further reaction.

After covalently attaching the tether-MAP to the amine-terminated surface [Fig. 2(a)], an increase in height of less than or equal to 25 Å for the coupling step was expected (11.4 Å for the homobifunctional crosslinker and 14 Å for the peptide based on the product data sheet and simple Chem3D models of the molecules), presuming a uniform packing of upright, optimized geometry peptide and crosslinker to the surface. Our values of 16–22 Å were consistent with this expectation. The slightly lower than maximum theoretical thickness is likely due to steric hindrance of the relatively bulky peptide on the surface inhibiting reaction with neighboring sites and charge repulsion between neighboring peptide molecules.

C. *cla*MP-link-MMP-8 fusion construct binding to peptide inhibitor

Once the peptide was coupled to the surface, the samples were incubated in protein solution, washed, and dried. The measured thicknesses for one concentration of *cla*MP-link-MMP-8 fusion construct on both the control and the amine-terminated SAMs are shown in Fig. 3.

For the control R-OH SAMs, no significant change in height throughout the course of these experiments was observed, which was expected because no crosslinking of the peptide should occur with surface hydroxyl groups and only nonspecific interactions between MMP-8 and the R-OH surfaces are possible. In the case of the R-NH_2 SAM, an increase in thickness was observed after the peptide coupling step as well as after MMP-8 incubation. This indicates that

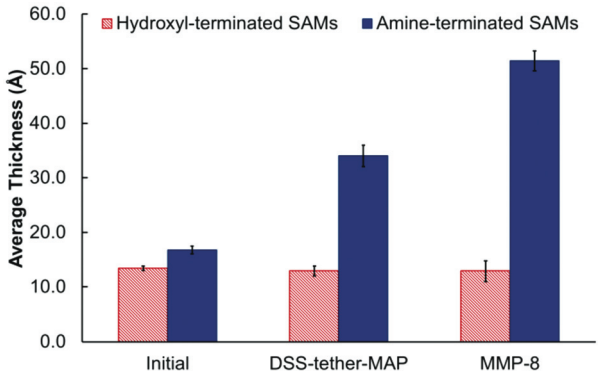

FIG. 3. Ellipsometric thickness for adsorption of 3.3 μM *cla*MP-link-MMP-8 fusion construct: (1) initial, (2) after peptide coupling, and (3) after MMP-8 incubation. Red hashed bars are R-OH samples, and blue solid bars are R-NH_2 samples. Error bars represent standard deviation of measurements of replicate samples (n = 3).

(1) the peptide is coupled to the amine surface and (2) the protein is indeed interacting with the peptide on the surface.

Addition of 3.3 μM MMP-8 to the peptide bound amine-terminated surfaces resulted in a large increase in height (~20 Å) supporting the idea that the peptide binds MMP-8 (Fig. 3) and is not simply abstracting metal from the MMP-8. A concentration dependent binding study was carried out with a series of different MMP-8 concentrations (0.1–3.3 μM from the same batch of protein with studies performed on the same day). For the amine-terminated SAMs with similar amounts of peptide grafted to the surface, a concentration dependent response was observed (Fig. 4). As the MMP-8 concentration was increased, an increase in the average thickness was observed. In this graph, the data have been plotted to show the thickness increase due to protein incubation relative to the peptide film. This response appears to level out at the higher concentrations, consistent with saturation of available binding sites.

D. MMP-8 fusion construct binding to peptide inhibitor

Although the data presented above are consistent with a direct and tight binding of MMP-8 to MAP, these studies were performed with an impure sample containing some fragments that may include the *cla*MP Tag. Potential interferences due to interactions of the *cla*MP Tag with the surface bound tether-MAP are expected to be reduced because the tag becomes occupied with nickel during purification of the fusion protein. Nonetheless, catalytically active MMP-8 fusion that does not encode the *cla*MP Tag was also tested after performing more extensive purification (and removal of fusion partner) to confirm that binding is neither due to contaminating fragments nor from degradation products. While degradation products and fragments are still present, they should be different in this second construct (MMP-8 fusion construct). In these studies, with normalization of peptide amount coupled to the surface, a very similar concentration dependent binding was observed (Fig. 5).

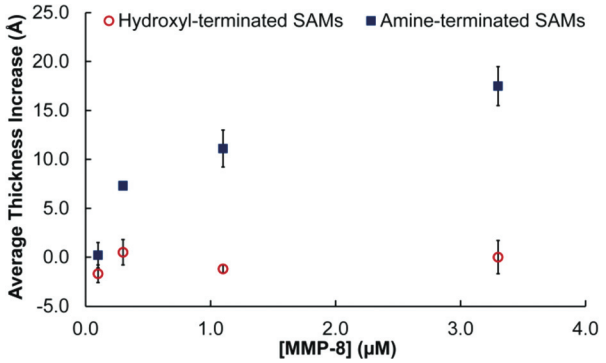

FIG. 4. Concentration dependent binding for *cla*MP-link-MMP-8 fusion construct. Red open circles (○) are for the R-OH control samples and the blue closed squares (■) are the R-NH_2 samples.

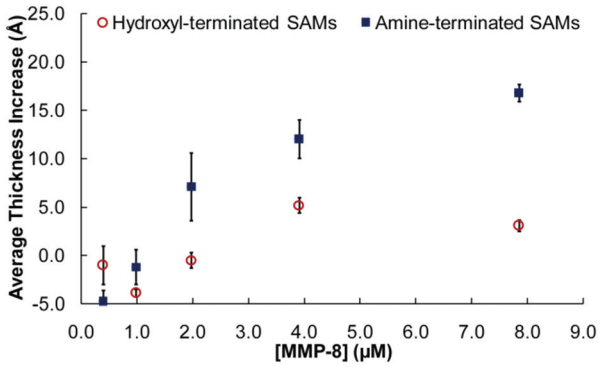

FIG. 5. Concentration dependent binding for MMP-8 fusion construct. Red open circles (○) are for the R-OH control samples, and the blue closed squares (■) are the R-NH_2 samples.

The MMP-8 fusion sample has increased purity compared to the *cla*MP-link-MMP-8 fusion construct, but it is less stable and degrades more significantly with time. This prevents the data from the two MMP-8 constructs from being compared quantitatively. Additionally, the MMP-8 fusion construct showed increased nonspecific adsorption at high concentrations on the hydroxyl-terminated control samples relative to the *cla*MP-link-MMP-8 fusion construct. However, the fact that the same trend in binding is observed with these two independent MMP-8 constructs provides strong evidence that MMP-8 is interacting with the peptide and forming a long-lived bound complex (on the time scale of these experiments) at the surface and that this thickness increase is not the result of nonspecific adsorption.

E. Removal of MMP-8 and Zn^{2+} binding to tether-MAP

Figure 6 shows an experiment similar to that shown in Fig. 3, at a different protein concentration (1.1 μM), but it also shows the results of experiments subsequent to the MMP-8 adsorption step. Repeated washing with denaturants and acetate buffers resulted in the successful removal of the protein as evidenced by the decrease in thickness. The decreased thickness is equivalent to the value observed prior to MMP-8 incubation as shown in step 4 of Fig. 6.

In order to ensure that the large increase in height observed upon MMP-8 incubation was due to an interaction with MMP-8 and not a result of a conformational change in the surface bound tether-MAP peptide due to zinc ion binding, we incubated the peptide modified SAMs in zinc ions (10–100 μM $ZnSO_4$ for ~30–120 min). After incubation in zinc ions, no significant change in height was observed (Fig. 6). This demonstrates that binding of the Zn^{2+} ions to the peptide would not provide a significant change in thickness, and therefore suggests that the tether-MAP is not merely abstracting the Zn^{2+} from the MMP-8 but rather interacting directly with the MMP-8.

To specifically investigate the role of the metal binding MAP Tag in the interaction between the surface bound peptide and the MMP-8, the tether-MAP was incubated with either zinc ions or nickel ions (10–100 μM $ZnSO_4$ or $NiSO_4$ for ~30–120 min) to block the MAP Tag on the peptide. After this blocking step, the thickness did not change significantly upon addition of either metal (Fig. 6). In either case, zinc or nickel ions, once the metal ions occupied sites on the surface a greatly decreased amount of MMP-8 binding was observed on the surface upon exposure to the MMP-8. In the case of the MMP-8 fusion construct, for the highest concentration of MMP-8 used (7.9 μM) without the metal blocking a thickness of 15.5 ± 0.9 Å was observed (Fig. 5). However, when the

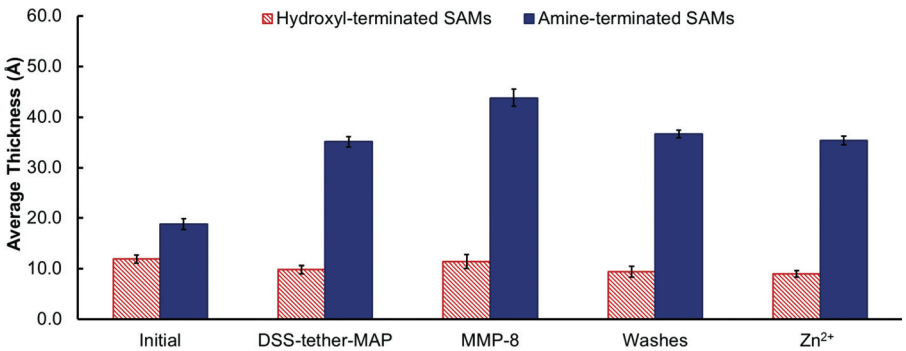

FIG. 6. Ellipsometric thickness for adsorption of 1.1 μM *cla*MP-link-MMP-8 fusion construct (1) initial, (2) after peptide coupling, (3) after MMP-8 incubation, (4) after protein removal with denaturant washes and acetate buffers, and (5) following Zn^{2+} incubation. Red hashed bars are R-OH samples and blue solid bars are R-NH_2 samples. Error bars represent standard deviation of measurements of replicate samples (n = 3).

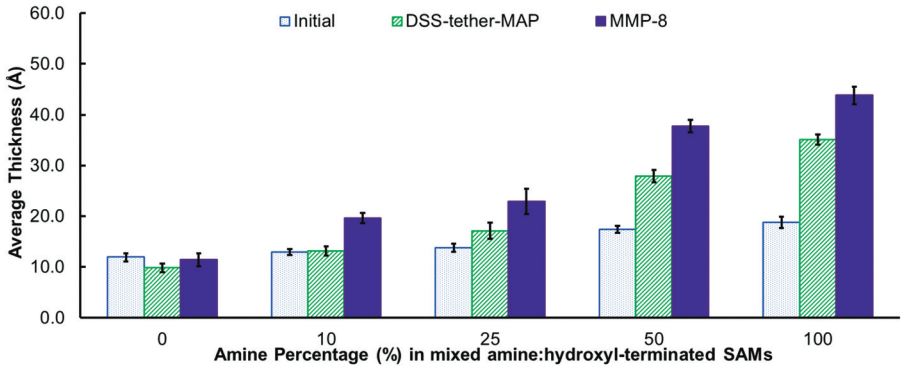

FIG. 7. Binding of tether-MAP and MMP-8 (*cla*MP-link-MMP-8 fusion construct) to mixed SAMs with various % amine. For each composition, three thicknesses are shown: (1) initial (blue dotted), (2) after peptide coupling (green hashed), and (3) after MMP-8 incubation (solid purple).

samples were preincubated in $NiSO_4$, an increase of only 1.7 ± 0.9 Å was observed for 7.9 μM MMP-8 solution. This indicates that the metal binding site of the MAP Tag is playing a critical role in the binding of the MMP-8, likely through interaction with the Zn^{2+} in the active site of the MMP-8. A very similar experiment was conducted on the *cla*MP-link-MMP-8 fusion construct with very similar results (not shown), again indicating that the results are not due to something specific about this particular MMP-8 construct.

F. Role of tether-MAP density in MMP-8 binding

The binding of the protein to surfaces with different amounts of peptide (created by using different amounts of amine) was also investigated. Mixed SAM films with different ratios of amine- and hydroxyl-termination were prepared and peptide coupling experiments carried out. Generally, the samples containing the most amine bound the most peptide and those samples with the most peptide bound the most MMP-8 as illustrated in Fig. 7. Interestingly, when MMP-8 binding studies were carried out on these surfaces with varying tether-MAP amounts, the 50% amine sample showed at least as much MMP-8 binding as the 100% amine sample even though the 100% amine sample showed the most peptide adsorption. This may be a result of steric interactions which block some of the peptide from being able to bind MMP-8 and suggests that the optimum density of the peptide for the binding experiments may be lower than that observed for the 100% amine-terminated SAMs used in this investigation.

IV. SUMMARY AND CONCLUSIONS

The mechanism of MMP-8 inhibition by the tether-MAP peptide was investigated using ellipsometry and two different MMP-8 constructs. After exposure of the peptide coupled surfaces to MMP-8, an increase in thickness was observed, suggesting a long-lived binding interaction between the two species. The blocking of the metal binding site in the tether-MAP peptide greatly reduced the binding interaction. These results, plus the ability to extract MMP-8 from the surface using acidic *p*H and chelators, strongly suggest that MMP-8 inhibition occurs through a mechanism involving the interaction between the MAP Tag and the Zn^{2+} active site in MMP-8. Understanding of the mechanism for MMP-8 inhibition by the tether-MAP peptide will contribute to the design of more potent MMP inhibitors and/or assays for MMP levels which are critically important in a variety of pathologic disease states.

ACKNOWLEDGMENTS

Funding was provided by NIH/NIDCR Grant No. R01-DE014392 and Collaborative Administrative Supplement DE022054-03 and by NIH COBRE P20 RR017708. Takeru Higuchi Predoctoral Fellowship and the NIH Chemical Biology Training Grant (T32GM008545) provided support for MLM. J.S.L. is co-owner of Echogen Inc., a limited liability company that has licensed the patent-protected metal abstraction peptide (MAP)/*cla*MP Tag technology from University of Kansas. All other authors declare that they have no conflicts of interest with the contents of this article.

[1]E. Dejonckheere, R. E. Vandenbroucke, and C. Libert, Cytokine Growth Factor Rev. **22**, 73 (2011).
[2]A. Gutiérrez-Fernández *et al.*, Cancer Res. **68**, 2755 (2008).
[3]E. Milia, E. Cumbo, R. Jose, A. Cardoso, and G. Gallina, Curr. Pharm. Des. **18**, 5542 (2012).
[4]M. Sulkala, T. Tervahartiala, T. Sorsa, M. Larmas, T. Salo, and L. Tjäderhane, Arch. Oral Biol. **52**, 121 (2007).
[5]J. M. Wells, A. Gaggar, and J. E. Blalock, Matrix Biol. **44–46**, 122 (2015).
[6]E. Hadler-Olsen, J.-O. Winberg, and L. Uhlin-Hansen, Tumor Biol. **34**, 2041 (2013).
[7]S. D. Shapiro, Curr. Opin. Cell Biol. **10**, 602 (1998).
[8]P. Spencer, Q. Ye, A. Misra, S. E. P. Goncalves, and J. S. Laurence, J. Dent. Res. **93**, 1243 (2014).
[9]M. A. R. Buzalaf, M. T. Kato, and A. R. Hannas, Adv. Dent. Res. **24**, 72 (2012).
[10]L. Tjäderhane *et al.*, Dent. Mater. **29**, 116 (2013).
[11]F. E. Jacobsen, J. A. Lewis, and S. M. Cohen, J. Am. Chem. Soc. **128**, 3156 (2006).
[12]J. Hu, P. E. Van den Steen, Q.-X. A. Sang, and G. Opdenakker, Nat. Rev. Drug Discovery **6**, 480 (2007).
[13]A. Tezvergil-Mutluay *et al.*, J. Dent. **39**, 57 (2011).
[14]M. W. Ndinguri, M. Bhowmick, D. Tokmina-Roszyk, T. K. Robichaud, and G. B. Fields, Molecules **17**, 14230 (2012).
[15]G. Dormán, S. Cseh, I. Hajdú, L. Barna, D. Kónya, K. Kupai, L. Kovács, and P. Ferdinandy, Drugs **70**, 949 (2010).
[16]N. Dixit, J. K. Settle, Q. Ye, C. L. Berrie, P. Spencer, and J. S. Laurence, J. Biomed. Mater. Res., Part B **103**, 324 (2015).

[17]M. L. McNiff, E. P. Haynes, N. Dixit, F. P. Gao, and J. S. Laurence, Protein Expression Purif. **122**, 64 (2016).
[18]H. Elwing, Biomaterials **19**, 397 (1998).
[19]K. L. Prime and G. M. Whitesides, J. Am. Chem. Soc. **115**, 10714 (1993).
[20]P. Tengvall, I. Lundström, and B. Liedberg, Biomaterials **19**, 407 (1998).
[21]H. Wang, S. Chen, L. Li, and S. Jiang, Langmuir **21**, 2633 (2005).
[22]A. G. Frutos, J. M. Brockman, and R. M. Corn, Langmuir **16**, 2192 (2000).
[23]M. Watanabe and K. Kajikawa, Sens. Actuators, B **89**, 126 (2003).
[24]C. Pale-Grosdemange, E. S. Simon, K. L. Prime, and G. M. Whitesides, J. Am. Chem. Soc. **113**, 12 (1991).
[25]B. Berron and G. K. Jennings, Langmuir **22**, 7235 (2006).
[26]R. C. Sabapathy and R. M. Crooks, Langmuir **16**, 1777 (2000).
[27]W. Pan, C. J. Durning, and N. J. Turro, Langmuir **12**, 4469 (1996).
[28]M. E. Krause, A. M. Glass, T. A. Jackson, and J. S. Laurence, Inorg. Chem. **50**, 2479 (2011).